The orientations of core antenna chlorophylls in photosystem II are optimized to maximize the quantum yield of photosynthesis

Sergei Vasil'ev[a,*], Jian-Ren Shen[b], Nobuo Kamiya[c], Doug Bruce[a]

[a]*Department of Biological Sciences, Brock University, St. Catharines, ON, Canada L2S 3A1*
[b]*Department of Biology, Faculty of Science, Okayama University, Okayama 700-8539, and PRESTO, JST, Saitama, Japan*
[c]*RIKEN, Harima Institute/Spring-8, Kouto 1-1-1, Mikazuki-cho, Sayou-gun, Hyogo 679-5148, Japan*

Abstract In photosystem II (PSII) the probability that energy absorbed by core antenna chlorophyll (Chl) is transferred to the reaction center (RC) is extremely high. Although close proximity between antenna Chl ensures a high transfer efficiency, relative pigment orientation can fractionally modify it. This level of refinement has often been assumed to be superfluous as so many subsequent processes limit the overall efficiency of photosynthesis. Nevertheless, did natural selection act on the most efficient step of energy conversion in PSII by optimizing the orientation of antenna Chl? Our Monte Carlo simulations sampled the orientation space of Chls in kinetic models for excitation energy transfer based on the X-ray structures of PSII from *Thermosynechococcus vulcanus* and *Synechocystis elongatus*. Our results revealed that the orientations of key antenna Chls are optimized to maximize photosynthesis while the orientations of the two peripheral RC Chls (ChlZ) are not. © 2004 Federation of European Biochemical Societies. Published by Elsevier B.V. All rights reserved.

Key words: Energy transfer; Photosystem II; Light harvesting

1. Introduction

Photosystem (PS) II is one of two photochemical reaction centers (RCs) that convert solar energy into stable chemical energy in oxygenic photosynthesis. The role of PSII in photosynthesis is to catalyze both the oxidation of water, with the resulting release of molecular oxygen, and the reduction of the mobile electron transport carrier plastoquinone.

In PSII a number of pigments act as light-harvesting antenna to absorb and direct solar energy to a single RC, where the charge separation that drives the chemistry of photosynthesis occurs. The effectiveness of the photochemical RC depends on the efficient transfer of excitation energy from these antenna molecules. Charge separation (formation of the primary radical pair P680$^+$ and Pheo$^-$) and charge stabilization (reduction of the primary quinone electron acceptor, Q$_A$) in PSII can occur with greater than 90% quantum efficiency [1]. Plants are challenged by having to function efficiently under light-limiting conditions and protect themselves from photodamage under conditions when light absorption exceeds metabolic demand. The relative number of antenna pigments that transfer excitation energy to the RC of PSII, and the efficiency of energy transfer between antenna and RC are critical factors in the balance between optimizing energy conversion and avoiding photodamage.

The RC of PSII consists of the D1 and D2 proteins, the PsbI protein, cytochrome b_{559} (Cyt b_{559}) and binds six chlorophyll (Chl) and two pheophytin (Pheo) molecules [2]. Two RC Chls, Chl$_Z$(D1) and Chl$_Z$(D2) are located at the periphery of the RC. One of these Chls appears to form part of a Cyt b_{559}-mediated cyclic electron transport pathway around PSII as it is ultimately oxidized by P680$^+$ and reduced by Cyt b_{559} which in turn is reduced by plastoquinone [3].

Associated with the RC are the oxygen-evolving complex (OEC) and two core antenna proteins, CP43 and CP47, that together contain approximately 30 Chls. Additional light-harvesting antenna proteins may increase the number of antenna pigments transferring energy to PSII. These include the Chls containing light-harvesting complexes in plants and green algae and the phycobilin proteins of red algae and cyanobacteria.

The recent solution of X-ray crystal structures for PSI [4] and PSII [5,6] has opened the door to an increasingly detailed understanding of photosynthetic function. Recent examination of the design of PSI has revealed that the quantum efficiency of this PS only weakly depends on the orientations of antenna Chls [7]. However, this work also showed that the existing arrangement of Chls in PSI is near optimal. The core antenna design of PSII is different from that of PSI. Instead of the ring of pigments around the RC seen in PSI, the Chl antennae of CP43 and CP47 in PSII form two clusters that flank the RC chromophores. The core antenna Chls of PSII are more distant from the RC than those in PSI, only a few of them are located within 30 Å of any of the RC chromophores. Structure-based excitation transfer calculations have shown that chromophores in CP43, CP47 and the RC form a three-compartment system, where energy transfer within each compartment is much faster than transfer between compartments [8,9]. How dependent is photosynthetic yield to changes in the arrangement of antenna Chls in PSII? From an evolutionary perspective another question arises. Are the orientations of the antenna Chls optimized in PSII for the highest yield of photosynthesis?

In this study we addressed the first question by Monte Carlo sampling of the orientation space of the antenna Chls and evaluating the yield of charge stabilization for each com-

---

*Corresponding author. Fax: (1)-905-688 1855.
E-mail address: svassili@brocku.ca (S. Vasil'ev).

Abbreviations: Chl, chlorophyll; PS, photosystem; RC, reaction center

bination of orientations. The second question was addressed by comparing the results of the random sampling of orientation space to the orientations identified in the two published X-ray structures of PSII.

2. Materials and methods

The X-ray structure of PSII from *Thermosynechococcus vulcanus* was refined based upon an electron density map that was improved by recalculations of reflection phases with newly obtained molecular masks from the previously published structural model [6]. The improved electron density map gave rise to clearer features for the phytyl tails of a number of the antenna Chls. There were also some Chls whose phytyl tails were found to be too close to a nearby protein or pigment residue based on the new electron density; the positions and/or orientations of these Chls were modified to ensure a stereochemically more reasonable structure. The refined structure fits better into the electron density map based on the combined phases, and thus represents an improvement over the originally published structure [6].

Kinetic models for excitation energy transfer between all pigments in PSII were constructed based on the X-ray structure of *Synechocystis elongatus* (1ILX.pdb) [8] and the refined X-ray structure of *T. vulcanus* discussed above. The excitation transfer rates between Chls were calculated based on Förster theory as described previously [10]. The P680 dimer was represented by an exciton. The lower excitonic state carried most of the oscillator strength and its energy was chosen to be $14\,630$ cm^{-1} [11]. The site energies for the remaining Chls were set at 675 nm ($14\,814$ cm^{-1}). The master equation, describing time evolution of excitation in the system along with all Chl sites, contained two additional sites representing the primary pheophytin electron acceptor, Pheo, and secondary quinone electron acceptor, Q$_A$. The yield of stable charge separation was calculated numerically as $\rho_{Q_A}(t)/\Sigma_i\rho_i(0)$ where ρ_{Q_A} denotes the probability that the quinone acceptor Q$_A$ is reduced and $\Sigma_i\rho_i(0)$ is the total amount of excitation at time zero. Unimolecular decay rates were 0.5 ns^{-1}, the index of refraction was 1.5 [12], the rate of charge separation was 1000 ns^{-1} and the rate of recombination 4.5 ns^{-1} [8].

Transition dipoles for each chromophore were located at the center of each chromophore as found in the appropriate X-ray structure. In some calculations the orientations of the transition dipoles of some or all of the antenna chromophores were randomized. To form the ensemble of random dipole orientations we first generated 4096 points uniformly distributed on a sphere of unit radius using the 'spiral' algorithm [13]. The ensemble was then formed by random independent selection of the dipole orientations from the set of 4096 points.

3. Results

Table 1 lists the positions and transition dipoles for antenna Chl molecules according to the refinement of the PSII structure of *T. vulcanus* described in Section 2. For most of the antenna Chls the changes in position and orientation with respect to the originally published structure are subtle. The most significant changes were for a number of Chls with altered transition dipoles. In all such cases the difference arose from a rotation of the transition dipole within the plane of the chlorine ring. The modified positions and dipole orientations associated with the revised structure, and shown in Table 1, were used for excitation energy dynamics calculations for *T. vulcanus* in place of those associated with the previously published structure, PDB entry 1IZL [6].

Fig. 1 overlays the structure of PSII for *T. vulcanus*, described in Section 2, with that of *S. elongatus* described by PDB entry 1ILX [8]. The positions of the PSII chromophores are very similar with some minor changes. 12 of the 13 Chls in CP43 observed in *T. vulcanus* are also present in the structure of *S. elongatus*. In both structures, these 12 Chls in CP43 all have symmetry-related analogs in CP47. One peripheral Chl that also has a CP47 analog was resolved only in the *S. elongatus* structure. Another one, which does not have a matching Chl in CP47, is observed only in the *T. vulcanus* structure. In addition, in both structures, three to four Chls are found only in CP47 with no matching analogs in CP43.

Table 1
The revised central Mg coordinates and transition dipoles of PSII antenna Chls

No.	Center			Transition dipole		
	X	Y	Z	X	Y	Z
12	51.452	35.256	49.948	−0.222028	−0.830495	0.510864
13	−7.409	67.198	44.613	−0.231463	−0.319474	0.918891
14	66.704	61.292	57.223	0.888713	−0.442247	−0.120861
15	33.980	67.296	71.408	−0.796407	0.597926	0.090670
16	42.915	71.758	61.474	−0.711835	0.684486	−0.157384
18	50.859	73.301	56.264	0.779711	−0.602662	−0.169848
19	53.852	59.613	73.206	0.445878	0.875859	−0.184561
20	50.909	71.606	74.429	0.351244	0.367650	−0.861082
21	44.769	64.161	67.184	−0.023089	0.371163	−0.928281
22	59.730	76.572	63.059	−0.898406	0.087752	−0.430310
23	43.922	70.019	49.815	−0.601105	−0.284904	−0.746661
24	59.072	87.520	63.007	0.751786	−0.521653	−0.403355
26	58.216	66.513	58.168	−0.390970	−0.918642	0.056918
27	−15.021	58.475	20.162	0.903060	0.245091	−0.352723
28	3.103	37.499	22.096	0.693253	0.666933	−0.273130
31	−20.281	31.591	22.599	−0.649422	−0.743084	−0.161486
32	−3.837	37.115	29.591	−0.808434	0.559589	0.182469
33	−15.390	41.528	27.966	−0.038021	−0.994018	0.102384
34	−9.995	31.075	23.347	−0.901490	−0.281110	−0.329080
35	−0.483	58.117	28.447	−0.722725	−0.078287	−0.686688
36	11.342	36.863	14.161	−0.408820	0.201181	−0.890164
37	−16.045	47.400	34.939	−0.907929	−0.281600	−0.310431
38	−9.363	43.662	9.437	0.971214	0.058884	0.230816
39	8.606	47.468	21.091	0.479662	0.455567	0.749922
41	−7.355	37.085	3.231	0.014674	−0.993831	−0.109928
42	−29.258	52.973	35.190	0.738408	0.137115	−0.660267
43	−15.594	31.552	12.670	−0.864644	−0.315048	0.391326

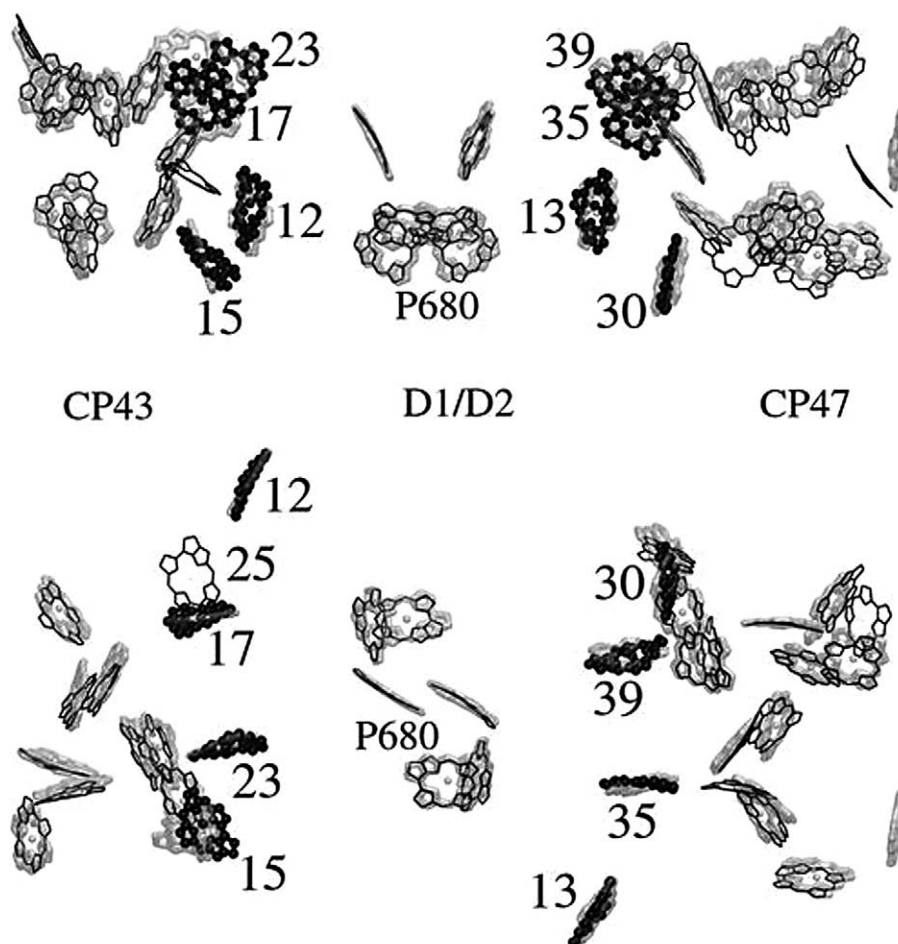The frame of reference is the same as in PDB entry 1IZL.

Fig. 1. Positions of the chromophores from the X-ray structures of PSII from *T. vulcanus* (black) and *S. elongatus* (gray). The top panel shows a view within the membrane plane, and the bottom panel shows a view normal to the membrane plane. Highlighted are the six bridging Chls (numbers 15, 17, 23, 30, 35 and 39) and the two Chl$_Z$s (numbers 12 and 13). The extra Chl in *T. vulcanus* is Chl number 25. Chl numbering is as in 1IZL.pdb. This figure was produced with VMD [17]. See text for details.

For both *T. vulcanus* and *S. elongatus* we generated an ensemble of PSII models with alternate arrangement of the transition dipoles by random independent orientation of the antenna Chls. We then assessed the quantum yield of photochemistry, as Q_A^- formation, of kinetic models for excitation energy transfer based on each of the resulting structural configurations. The results of simulations are represented as histograms of the yield distribution (Figs. 2–4). The number of scores in each histogram bin is equal to the number of Chl arrangements for which the quantum yield of photochemistry falls within the range of the bin. The area under the entire histogram represents the total number of occurrences of all possible yields, which is also the total number of different structural configurations tested. For all trials this number was at least 10^7. The histograms were used to calculate the probability of occurrence of any particular quantum yield.

3.1. Randomizing all of the antenna Chls in PSII

Fig. 2 shows histograms of quantum yield of the ensembles formed by random independent orientation of all 30 antenna Chls and the two Chl$_Z$s for both *T. vulcanus* and *S. elongatus*. The peaks of the distributions are at 94.2 and 94.5% and the halfwidths of the distributions are 1.2 and 0.7% for the *S. elongatus* and *T. vulcanus* structures, respectively. The total

span of either distribution is about 4.5%. It is seen that for both structures, the observed X-ray Chl arrangement is nearly at the middle of the distribution, 32–34% of randomly generated arrangements have a better quantum yield. Two conclusions can be drawn from these data:

1. The quantum yield calculated using the observed X-ray arrangement is somewhat shifted toward the higher end of the distribution indicating a slight trend toward optimization.
2. The whole PSII antenna aggregate is not nearly as optimized as was previously shown for the entire PSI antenna aggregate [7].

An immediate question arises from this result: is the lack of pronounced optimality a characteristic of all Chls in the PSII antenna system? Are there any functional groups of pigments within PSII that are optimized? To identify such optimized pigment clusters, we first considered the set of pigments closest to the RC. These Chls are expected to have the most significant influence on the overall energy transfer rate from antenna to the RC and on its quantum yield [2].

We select this set of pigments using a 29 Å cut-off distance from the closest pigment in the RC core. This distance roughly corresponds to a 10-fold decrease of the rate of energy transfer from its maximal value determined for the Chls
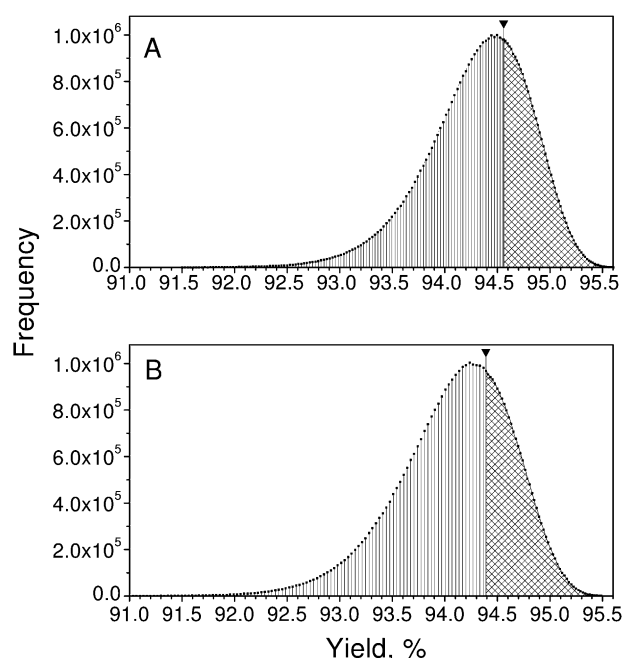
Fig. 2. Histograms of the yield of charge stabilization distribution constructed from Monte Carlo simulations (see Section 2 for details). Transition dipole orientations of all 30 antenna Chls and two Chl$_Z$s were sampled randomly. A: *T. vulcanus* structure. B: *S. elongatus* structure. Down triangles mark X-ray dipole orientations.

closest to the core pigments (Chls 24 and 42 in PDB file 1ILX). Pigments outside this range are not likely to have a significant effect on the overall energy transfer rate from antenna to the RC. Nine Chls (numbers 12, 13, 15, 17, 23, 25, 29, 30, and 35) were found within this cut-off in the *T. vulcanus* structure, and eight Chls (numbers 19, 20, 22, 24, 30, 37, 42, and 46) in the *S. elongatus* structure. These Chls are highlighted in Fig. 1 and belong to two different functional groups. The first group includes six bridging light-harvesting antenna Chls located in CP43 (numbers 22, 24, 30 in 1ILX; 15, 17, 23 in 1IZL) and CP47 (numbers 37, 42, 46 in 1ILX; 30, 35, 39 in 1IZL). The second group contains two redox active Chls, Chl$_Z$(D1) and Chl$_Z$(D2), located in the RC subunits and coordinated by D1-His118 and D2-His117 [3]. The one 'extra' Chl (number 25 in 1IZL) located between Chl$_Z$(D2) and CP43 Chl and observed only in the *T. vulcanus* structure, has previously been suggested to participate in the alternative electron transfer pathway involving Chl$_Z$ [14]. This Chl was analyzed separately (data not shown).

3.2. Antenna bridging Chls

The yield distributions calculated for the random ensembles of the six antenna bridging Chls common to the *T. vulcanus* and *S. elongatus* structures are shown in Fig. 3. As expected the widths of these distributions were smaller than for the ensembles in which the orientations of all antenna Chl were randomized, but not by much. These six Chls are thus responsible for much of the variation in quantum yield observed when all antennae are randomized. However, in contrast with the histograms generated by randomizing all antennae, it is clear that the orientations of these six Chls as found in the X-ray structures of both *T. vulcanus* and *S. elongatus* are nearly optimal for maximizing the quantum yield of PSII.

Only 1.31% of random orientations have a higher quantum yield than the X-ray determined orientations in *T. vulcanus*, and only 1.66% in *S. elongatus*.

When comparing the transition dipole orientations of Chls in *T. vulcanus* (as shown in Table 1) with those in *S. elongatus* it is apparent that although five of these six bridging Chls have very similar transition dipole orientations in both structures, one does not. The transition dipole of Chl 37 in *S. elongatus* is oriented at approximately 90° to that of its equivalent, Chl 30, in *T. vulcanus*. However, in a 3.6 Å resolution unpublished structure of *S. elongatus* (Petra Fromme, personal communication) the transition dipole orientations of all six bridging Chls agree with the revised structure of *T. vulcanus* (as shown in Table 1). The quantum yield of the *S. elongatus* kinetic model was increased when the transition dipole of Chl 37 was rotated to match the unpublished *S. elongatus* structure. Only 0.78% of all random orientations had a higher quantum yield than this modified *S. elongatus* structure. Our results for both *T. vulcanus* and *S. elongatus* indicate that the orientations of the bridging antenna Chls closest to the RC have been strongly selected over the course of evolution to maximize the quantum yield of PSII.

3.3. Chl$_Z$ and the 'extra' Chl

Both Chl$_Z$s are located at a distance of less than 25 Å from the RC core chromophores. The results of our study show that in contrast to the antenna bridging Chls, the orientations of both Chl$_Z$(D1) and Chl$_Z$(D2) are not optimal (Fig. 4). Interestingly, only 14% (*T. vulcanus*) and 6.4% (*S. elongatus*) of random orientations had a lower quantum yield than the orientations found in the X-ray structures. This suggests that the orientation of these two Chl$_Z$s may have been optimized for purposes other than efficient transfer of excitation energy to the RC core. The same motif was found for the 'extra' Chl
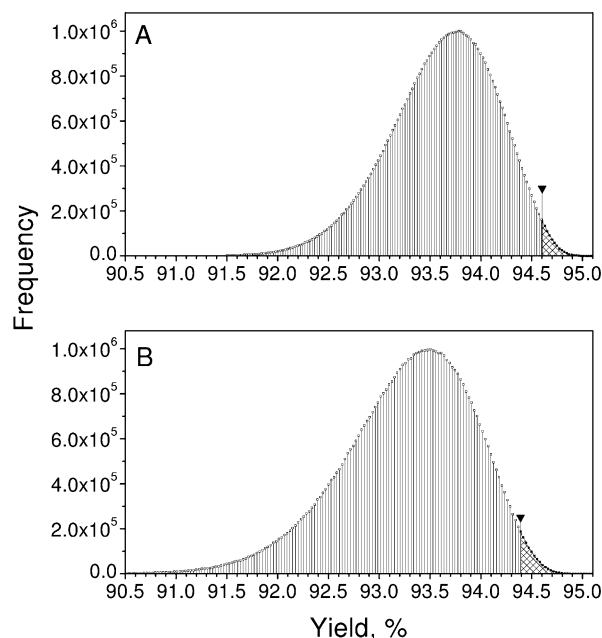

Fig. 3. Histograms of the yield of charge stabilization distribution constructed from Monte Carlo simulations. Transition dipole orientations of six bridging Chls were sampled. A: *T. vulcanus* structure. B: *S. elongatus* structure. Down triangles mark X-ray dipole orientations. Details of simulation as described in Section 2.
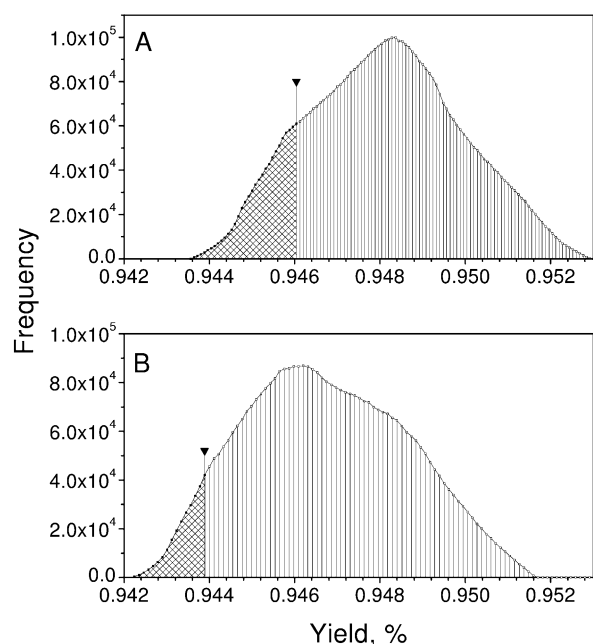
Fig. 4. Histograms of the yield of charge stabilization distribution constructed from Monte Carlo simulations. Transition dipole orientations of the two Chl$_Z$s were sampled for *T. vulcanus* structure (A) and *S. elongatus* structure (B). Down triangles mark X-ray dipole orientations. Details of simulation as described in Section 2.

of CP43, which was only described in the *T. vulcanus* structure (data not shown).

4. Discussion

We have found that the orientations of bridging antenna Chls are near optimal for maximizing the quantum yield of photochemistry in PSII. Recently, a similar simulation was reported that analyzed the arrangement of all antenna Chls of PSI [7]. Results of that work revealed light harvesting in PSI to be optimized as well. Optimality thus appears to be a common feature of core Chl antennae in oxygenic photosynthetic systems. If we estimate the potential gain in yield achieved by orientational optimization to be the optimal quantum yield minus the most probable quantum yield, we find a fairly modest gain in PSII (less than 1.3%). In the case of PSI the gain was previously shown to be even smaller, only about 0.3% [7]. Any such increase in photochemical efficiency will only be translated into an increase in the overall rate of photosynthesis under light-limiting conditions. In natural environments photosynthetic organisms are often limited by one or more of a number of different factors. Small increases in photochemical efficiency in the RC would thus, on average, lead to much smaller increases in photosynthetic productivity. Nevertheless, it appears that the advantage of increasing photosynthetic efficiency by at most 0.3–1% was sufficient for natural selection in this direction.

The degree of optimization obtained for these bridging Chls is especially significant when physical constraints affecting the possible positions of antenna Chl molecules are considered. Orientational constraints are expected to arise from considerations of assembly, structural stability and interaction with other photosynthetic components. Our orientational sampling protocol had no constraints and thus gives an overestimate of

the range of possible orientations. Regardless of this, the six bridging pigments were found to be strongly optimized within this overestimated range of possible orientations. Clearly the selection pressure for optimization of primary photochemistry was stronger than the selection pressures for any other factors constraining the positions of these bridging pigments.

In stark contrast were our findings for the two Chl$_Z$ molecules, whose orientations minimized their contribution to light harvesting. At present we do not know whether an unfavorable orientation for energy transfer is a requirement for the efficient function of these Chls as alternative electron donors to P680 or if it arises from an as yet unknown evolutionary constraint. The optimal orientation for energy transfer would have the transition dipole vector pointing towards the center of the RC core complex. The macrocycle planes of both Chl$_Z$s are almost normal to the direction of the optimal dipole vector. Thus, a major reorientation of the Chl plane would be required to orient the Chl$_Z$ optimally for energy transfer to the RC. Interestingly, Chl homologous to the two Chl$_Z$s have been found in PSI and in RCs of the putative PSI and PSII ancestors, green sulfur bacteria and heliobacteria [15,16]. The later finding indicates that Chl$_Z$ analogs appeared early in evolution and for some reason have been conserved in all of the above-mentioned organisms. The molecular function of Chl$_Z$ analogs in PSI and in the RCs of green sulfur bacteria and heliobacteria is not clear at present. They may have been important for energy transfer from light-harvesting antennae to the RCs early in evolution when pigment number and arrangement were different.

In conclusion, we have found in the present study that pigments in PSII can be divided into two groups depending on their orientational optimization for energy transfer efficiency. A group of six antenna Chls are highly optimized for bridging energy transfer between CP47 and CP43 and the RC chromophores. In contrast, the orientations of the two Chl$_Z$s in PSII appear to have been selected to minimize energy transfer to the RC. A more detailed study of orientation optimality of all individual Chls in both PSII and PSI may help to identify common evolutionary related blocks within these PSs and possibly shed some light on the nature of the selection pressures responsible for these differences.

References

[1] Hou, J.-M., Boichenko, V.A., Diner, B.A. and Mauzerall, D. (2001) Biochemistry 40, 7117–7125.
[2] Diner, B.A. and Rappaport, F. (2003) Annu. Rev. Plant Biol. 53, 551–580.
[3] Stewart, D.H., Cua, A., Chisholm, D.A., Diner, B.A., Bocian, D.F. and Brudvig, G.W. (1998) Biochemistry 37, 10040–10046.
[4] Jordan, P., Fromme, P., Witt, H.-T., Klukas, O., Saenger, W. and Krauß, N. (2001) Nature 411, 909–917.
[5] Zouni, A., Witt, H.-T., Kern, J., Fromme, P., Krauß, N., Saenger, W. and Orth, P. (2001) Nature 409, 739–743.
[6] Kamiya, N. and Shen, J.-R. (2003) Proc. Natl. Acad. Sci. USA 100, 98–103.
[7] Sener, M.K., Lu, D.Y., Ritz, T., Park, S., Fromme, P. and Schulten, K. (2002) J. Phys. Chem. B 106, 7948–7960.
[8] Vasil'ev, S., Orth, P., Zouni, A., Owens, T.G. and Bruce, D. (2001) Proc. Natl. Acad. Sci. USA 98, 8602–8607.

[9] de Weerd, F.L., van Stokkum, I.M., van Amerongen, H., Dekker, J.P. and van Grondelle, R. (2003) Biophys. J. 82, 1586–1597.

[10] Vasil'ev, S., Lee, C.-I., Brudvig, G.W. and Bruce, D. (2002) Biochemistry 40, 12236–12243.

[11] Smith, P.J., Peterson, S., Masters, V.M., Wydrzynski, T., Styring, S., Krausz, E. and Pace, R.J. (2002) Biochemistry 41, 1981–1989.

[12] Gruszecki, W.I., Grudzinski, W., Banaszek-Glos, A., Matula, M., Kernen, P., Krupa, Z. and Sielewiesiuk, J. (1999) Biochim. Biophys. Acta 1412, 173–183.

[13] Saff, E. and Kuijlaars, A. (1997) Math. Intell. 19, 5–11.

[14] Vasil'ev, S., Brudvig, G.W. and Bruce, D. (2003) FEBS Lett. 543, 159–163.

[15] Baymann, D., Brugna, M., Muhlenhoff, U. and Nitschke, W. (2001) Biochim. Biophys. Acta 1507, 291–310.

[16] Fyfe, P.K., Jones, M.R. and Heathcote, P. (2002) FEBS Lett. 530, 117–123.

[17] Humphrey, W., Dalke, A. and Schulten, K. (1996) J. Mol. Graph. 14, 33–38.